CHANGES AND IMPROVEMENTS IN THE CONSTRUCTION OF LARGE CASSEGRAIN ANTENNAE WITH PARABOLIC HORNREFLECTOR FEEDS

Änderungs- und Verbesserungsmoglichkeiten im Aufbau grosser Cassegrainantennen mit Hornparabolspeisung

by

G. v. Trentini, K. P. Romeiser, R. Reitzig

Central Laboratory for Communications Engineering,
Siemens AG, Munich, Germany

Frequenz
1968, Vol. 22, No. 8, p. 216-223

Translated by SCITRAN (Scientific Translation Service),
P. O. Box 5456, Santa Barbara, California 93103
on 1 September 1970.

Prepared for and issued by the Jet Propulsion Laboratory,
California Institute of Technology, Pasadena, Calif.,
under NASA contract NAS 7-100

CHANGES AND IMPROVEMENTS IN THE CONSTRUCTION OF LARGE CASSEGRAIN ANTENNAE WITH PARABOLIC HORNREFLECTOR FEEDS*

G. v. Trentini, K. P. Romeiser, R. Reitzig

Central Laboratory for Communications Engineering,
Siemens AG, Munich, Germany.

PART 3: Beam Equalization (R. Reitzig)

Abstract

The superposition of the TE_{11}- and TM_{11}-circular waveguide modes with the appropriate relative amplitude and phase in the aperture of a horn-reflector antenna causes beamwidth equalization and sidelobe suppression of from 17 dB to more than 30 dB in the electric plane. The TM_{11}-mode is set up at the junction of two circular wave-guides of different cross-section. A theoretical analysis of the mode-conversion and the dimension of the cross-sectional discontinuity for the condition of a rotational-symmetric distribution of the radiation field are presented. In addition, measurements of the far-field radiation pattern and the near-field distribution of the amplitude and the phase are given. The radiation characteristics of the TM_{01}- and TE_{01}-circular waveguide modes required for antennae tracking purposes are also investigated.

---

*Detailed version of three papers given on October 18th, 1967 in Darmstadt at the NTG-URSI Conference on antennae and electromagnetic fields.

Documentation Key Words

Low-noise feed system for a cassegrain antenna/ Near-field feeds/ Beam equalization/ TE_{11} and TM_{11} mode superposition in a circular waveguide/ Cross-section discontinuity in the circular waveguide.

3.1 INTRODUCTION

A circular hornreflector is usually excited by the TE_{11} fundamental mode of a circular waveguide feed. The resulting field distribution in the aperture of the hornreflector does not have rotational symmetry. Considerable deviations in the amplitude and phase distribution of the beam characteristic will therefore arise in various planes perpendicular to the aperture, in particular those with large hornreflectors. The position of the phase center of a circular hornreflector on two orthogonal sections moves toward the inside of the horn with increasing aperture size so that the phase center in the E-plane moves to larger depths [1]. The situation is similar for the beam width: narrowing of the beam characteristic in the far-field is more pronounced in the E-plane than in the orthogonal H-plane. The sidelobe levels exhibit a similar variation.

If a circular hornreflector is used as feed for a cassegrain antenna, then the receiver reflector and therefore the main reflector are not illuminated homogeneously in the various planes. The design of a circular receiver reflector requires that a compromise be made. A large receiver, suitable for the large divergence of the H plane, occults the central radiation of the main reflector to a large degree and therefore results in a gain reduction and an increase in the forward sidelobe. A small receiver reflector, suitable for the lower divergence of the feed system in the E-plane, increases the beam spillover in the other planes as well as the amount of scattered radiation. A compromise solution for the shape of the receiver reflector is also necessary due to the different positions of phase centers in the various section planes.

Potter [2] was able to eliminate these disadvantages by means of an additional TM_{11}-mode wave. He obtained a main lobe of the beam characteristic with perfect rotational symmetry, full coincidence of the phase centers in the E and H planes, and a sidelobe suppression of more than 30 dB.

It is natural to apply the same principle to paraboidal horn antenna. Sidelobe suppression is important, e.g. for radio relay engineering.

When the parabolic horn antenna is used as near-field feed for a large cassegrain antenna, e.g. in satellite ground stations, then an amplitude distribution with rotational symmetry allows us to select the optimum receiver illumination independent of the polarization. Beam reversal at the parabolic reflector transforms the phase center point of the spherical wave in the linear horn section into an extended phase front with rotational symmetry. An optimum correction of the receiver reflector contour is thus possible.

3.2 PROBLEM DEFINITION

The principle of cross-section symmetrization due to the simultaneous emission of the TE_{11} and TM_{11} mode is based on the interference of two waves with different propagation characteristics, and is therefore frequency dependent. The expected band width is important for a practical application.

Existing radio relay links (earth-satellite) operate at a receiver frequency in the 4 GHz range, while the transmission frequency lies in the 6 GHz range, i.e., higher by a factor of 1.5. Wavemode superposition can be optimized for only one frequency range. It is therefore necessary to study the variation of beam characteristics in the other frequency range as well as any possible compensation.

In the case of an automatic tracking device for a large reflector antenna, the error signal was determined most easily by eliminating the de-coupling of suitable waveguide modes, e.g. the TM_{01} and the

TE_{01} modes [3]. In order to apply this procedure for error signal determination to a system which is excited according to the dual-mode principle, we must first determine whether the TE_{11} - TM_{11} mode conversion mechanism has any effect on the directional characteristics of the TM_{01} and TE_{01} wave modes.

The present paper is largely concerned with the study of these problems. We report experimental results of a parabolic x-band horn antenna as well as the results of some theoretical investigations.

3.3 DESCRIPTION OF THE TEST DEVICE

The parabolic horn antenna studied here is illustrated in Figure 3.1. It consists of a round cone with an aperture angle of 15°; a parabolic reflector section (the focal point of which coincides with the cone tip) and a cylinder perpendicular to the cone axis with a diameter of D = 500 mm. An adapter is attached on the narrow end of the cone; it can be rotated around the cone axis and connects the cone with an x-band circular waveguide. The axial coupling allows us to set any desired polarization within the feed waveguide. The adapter is selected for each experiment, i.e. a conical waveguide adapter or a so-called dual-mode converter, both having a cone opening angle of 15°.

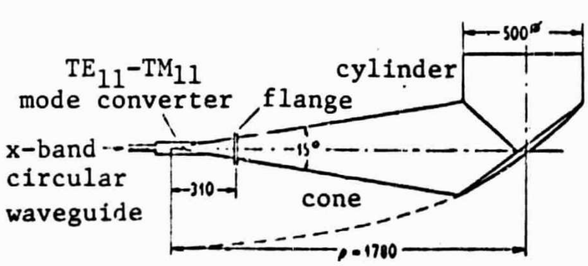

Figure 3.1. Design of the parabolic horn antenna.

The dual-mode converter (figure 3.2) is a conical waveguide with an axially symmetrical discontinuity in the cross-section. It is dimensioned so that only the TE_{11} fundamental mode can propagate in the narrow section of the waveguide; it is excited by the TE_{11} wave at the cross-section discontinuity. All other wave modes which may also be generated at the discontinuity are

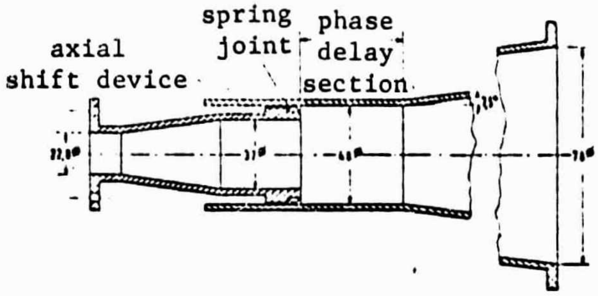

Figure 3.2. TE_{11} - TM_{11}-mode converter (Test construction for 8.2 GHz).

aperiodically damped. The condition of rotational symmetry in the radiation field characteristic requires a definite amplitude ratio of TE_{11} and TM_{11} modes. Section 4 contains an attempt to provide an approximate calculation of this amplitude ratio. The mode conversion is proportional to the size of the cross-section discontinuity and the frequency. A theoretical study of the wave mode conversion at the cross-section discontinuity is also included in Section 4.

The propagation velocities of the two wave modes are different and the relative phase is therefore a function of position. A common cylindrical phase tube behind the cross-section discontinuity is movable in the axial direction and allows one to set the correct phase condition at the beam aperture. The dispersion of TE_{11} and TM_{11} modes is largest near this region. The limiting wavelength for both modes increases steadily in the adjacent conical section of the paraboloidal horn antenna. The frequency dependence of the phase between TE_{11} and TM_{11} modes in the beam aperture is essentially determined by the cylindrical tube section behind the discontinuity for large cone angles. A change of the phase delay length by full multiples of the interference wave length between TE_{11} and TM_{11} waves produces a phase rotation in multiples of 2π. The measured characteristics for these discrete positions were found to be identical. This result is important for practical applications. A change of the phase delay length by multiples of the interference wave length for the optimum frequency makes it possible to control the radiation characteristic for a significantly higher frequency because of the correspondingly larger interference wavelength.

The reflection of the TE_{11} mode at the cross-section discontinuity must be compensated for by axially symmetrical circular baffles in the waveguide section. Rules for the dimensions of these compensation baffles have been described in [4].

3.4 APPROXIMATE DETERMINATION OF THE CROSS-SECTION DISCONTINUITY IN THE DUAL-MODE CONVERTER

It is known that there is a close physical correlation between the radiation field and the aperture field. Rotational symmetry of the three-dimensional radiation characteristic of the TE_{11} mode is obtained when the energy distribution in the aperture of the horn-reflector has rotational symmetry.

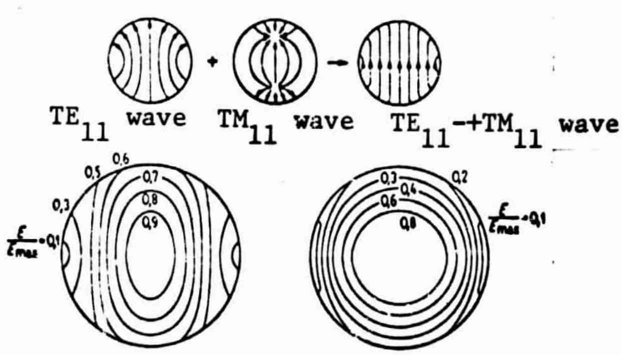

Figure 3.3 Transverse field distribution and curves of constant amplitude within the beam aperture.

Figure 3.3 shows the transverse electric field of the TE_{11} wave and its amplitude distribution in the antenna aperture. A superposition of the TE_{11} and TM_{11} waves with proper amplitude and phase relations shows that the requirement of energy distribution with rotational symmetry is fulfilled to a good approximation. A comparison with the TE_{11} distribution indicates that the sidelobe in the E plane is strongly suppressed. Actual measurements of the far field (see Section 5) show that sidelobe suppression is significantly improved. The nearly linear polarization of the resulting aperture field suggests a large reduction in the amount of transverse polarization. Measurements have indeed shown an improvement by approximately 10 dB. In the determination of the amplitude distribution of the resulting aperture field for Figure 3.3, we have assumed that the diameter D = 2A of the antenna aperture is significantly larger than the operational wavelength. With this requirement there is no significant difference between the phase velocities of the TE_{11}

and TM_{11} modes, and it is sufficient to a good approximation to consider only the transverse electric fields for both wave modes.

If δ is the complex amplitude ratio of TE_{11} and TM_{11} waves, and E_t^h and E_t^e are the normalized amplitudes of the transverse electric fields for both modes, then the superposed transverse electric field is, in general,

$$E_t = E_t^h + \delta E_t^e \tag{1}$$

After a substitution of suitable expressions for the field components in polar coordinates [4], we obtain:

$$E_r = \left[\frac{\frac{1}{r} J_1\left(\chi_h \frac{r}{A}\right)}{\sqrt{\frac{\pi}{2}} J_1(\chi_h) \sqrt{\chi_h^2 - 1}} + \delta \frac{J_1'\left(\chi_e \frac{r}{A}\right)}{\sqrt{\frac{\pi}{2}} \chi_e J_0(\chi_e)} \right] \sin\varphi = f_1(r) \sin\varphi$$

$$E_\varphi = \left[\frac{J_1'\left(\chi_h \frac{r}{A}\right)}{\sqrt{\frac{\pi}{2}} J_1(\chi_h) \sqrt{\chi_h^2 - 1}} + \delta \frac{\frac{1}{r} J_1\left(\chi_e \frac{r}{A}\right)}{\sqrt{\frac{\pi}{2}} \chi_e J_0(\chi_e)} \right] \cos\varphi = f_2(r) \cos\varphi. \tag{2}$$

The requirement of an aperture distribution with rotational symmetry demands that the functions $f_1(r)$ and $f_2(r)$ be identical. When both modes are in phase at the antenna aperture, then δ is obtained by the requirement of minimum difference between these two functions:

$$\int_{\varphi=0}^{2\pi} \int_{r=0}^{A} [f_1(r) - \delta f_2(r)]\, r\, dr\, d\varphi = 0. \tag{3}$$

The numerical evaluation results in $\delta = 0.38$.

The assumption $A \gg \lambda$ means that the amplitude ratio of the two modes is independent of frequency. This assumption is not fulfilled at the feed waveguide. In this case the wavelengths and the waveguide diameter have comparable orders of magnitude, and the mutually orthogonal TE_{11} and TM_{11} modes show significnat differences in their propagation behavior. The time-averaged energy transport of the TE_{11} wave is:

$$P_h = \frac{1}{2} \frac{a_h^2}{Z_h} \tag{4}$$

and that of the TM_{11} wave is: $P_e = 1/2\ a_e^2 Y_e$ where

$$Z_h = \frac{Z_0}{\sqrt{1-\left(\frac{\chi_h}{ak}\right)^2}} \quad \text{and} \quad Y_e = \frac{1}{Z_0} \frac{1}{\sqrt{1-\left(\frac{\chi_e}{ak}\right)^2}} \tag{5}$$

represent the characteristic impedance of the TE_{11} mode with amplitude a_h and the characteristic admittance of the TM_{11} mode with amplitude a_e, respectively. Both refer to a waveguide with diameter 2a at a frequency

$$f = \frac{k}{2\pi\sqrt{\varepsilon\mu}}$$

The TE_{11} and TM_{11} waves are mutually orthogonal so that the energy ratio δ^2, which is required for a field distribution in the antenna aperture with rotational symmetry, is maintained in the feed waveguide. Therefore one obtains

$$\delta^2 = \frac{P_e}{P_h} = \frac{a_e^2}{a_h^2} Y_e Z_h.$$

The amplitude ratio of both wave modes at the discontinuity within the feed waveguide is found to be:

$$\frac{a_e}{a_h} = \frac{0{,}38}{\sqrt{Y_e Z_h}}. \tag{6}$$

Equation (6) is illustrated in Figure 3.4. The amplitude ratio a_e/a_h for a given frequency approaches the value δ asymptotically with increasing waveguide diameter.

As a next step we have to determine the size of the cross-section discontinuity in the feed waveguide from the known amplitude ratio of the two wave modes. It is therefore necessary to have analytical expressions for the mechanism of TE_{11}/TM_{11} mode conversion. A detailed description of the physical principles of wave mode

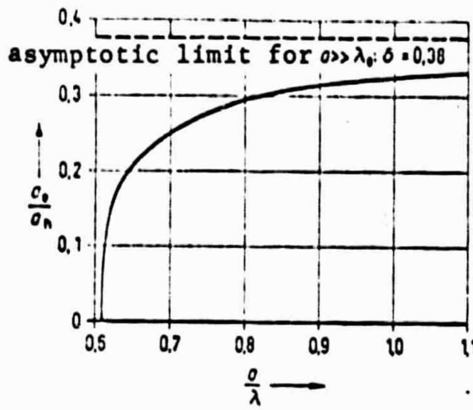

Figure 3.4 Amplitude ratio a_e/a_h of TE_{11}- and TM_{11} modes within the feed waveguide for aperture field distributions with rotational symmetry.

conversion at a cross-section discontinuity and the derivation of continuity relations of the transverse electric and magnetic fields at the discontinuity are given in [4].

The results given in the latter reference will be used for an approximate determination of the size of the cross-section discontinuity. An exact solution is not possible because of the required computational effort. In a first approximation, sufficient for practical applications, we will consider only the TE_{11} and TM_{11} modes.

Measurements have shown that it is sufficiently accurate to describe the field in the aperture plane of the cross-section discontinuity by only two types of waves. The exact diameter ratio must be determined by experiments for each case.

The amplitude ratio can be written approximately as:

$$\frac{a_e}{a_h} \approx \frac{\oint (\bar{z} \times \nabla_t \psi_e^A)\, \bar{n}\, \psi_h^B\, b\, d\varphi}{\left(\frac{\chi_h}{b}\right)^2 \int\limits_{\varphi=0}^{2\pi} \int\limits_{r=0}^{a} \psi_h^A\, \psi_h^B\, r\, dr\, d\varphi} =$$

$$= \frac{\sqrt{\chi_h^2 - 1}\; J_1(\chi_h)\, J_1\left(\chi_e \frac{b}{a}\right) \left[1 - \left(\frac{b}{a}\right)^2\right]}{\chi_e J_0(\chi_e) \left[\left(\chi_h \frac{b}{a}\right) J_0\left(\chi_h \frac{b}{a}\right) - J_1\left(\chi_h \frac{b}{a}\right)\right]} \qquad (7)$$

where the limits of integration are given by the boundary condition of the transverse electrical fields in the plane of discontinuity. The eigenfunctions ψ^B and ψ^A describe the field distribution within the narrow section of the waveguide (diameter 2b) and within the adjacent wider waveguide section (diameter 2a), respectively.

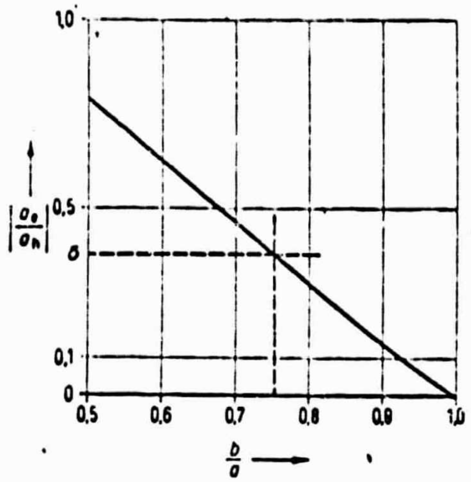

Figure 3.5. Amplitude ratio of TM_{11} and TE_{11} mode conversion as a function of the ratio of the diameters of two cylindrical waveguides.

Figure 3.5 illustrates Equation (7). The result is frequency-independent, since high-order wave modes have been neglected. The value δ = 0.38 for a radiation field distribution with rotational symmetry results in a diameter ratio of b/a = 0.75. A correction according to Equation (6), which includes at least the frequency dependence of the required amplitude ratio, results in b/a = 0.85 for f = 8.2 GHz and a = 24 mm. The correct value is probably between these two results. An experimental determination of the diameter ratio of both circular waveguides resulted in a radiation pattern with rotational symmetry for both the linear hornreflector and the parabolic horn antenna at f = 8.2 GHz for a value b/a = 0.77.

3.5 MEASUREMENT OF THE FAR-FIELD CHARACTERISTICS

The far-field characteristic of the parabolic antenna described in Section 3 was measured for various positions and directions of polarization in two frequency ranges, separated by a factor of 1.5 in the E-, H- and the 45°-planes. It was found that the high D/λ ratio of the antenna aperture made the resulting patterns essentially independent of position in regions near the axis which are of interest here. As an illustration of the measurement results, we have arbitrarily selected in the following figures the case of vertically polarized radiation incident on the aperture of a parabolic antenna with the cone tip directed upward.

In order to evaluate the radiation characteristics of a parabolic horn antenna with dual-mode excitation, we need to know the radiation patterns for conventional TE_{11} radiation. These distributions are shown in Figure 3.5 for f = 8.2 HGz and in Figure 3.6 for f = 12.4 GHz.

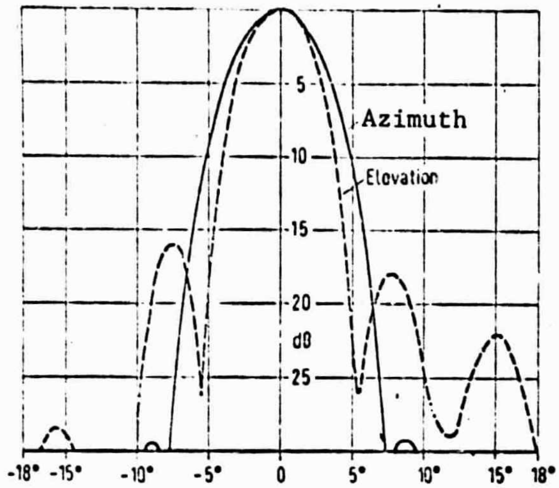

Figure 3.6. TE_{11} radiation characteristic of a parabolic horn antenna. Vertical polarization; f = 8.2 GHz.

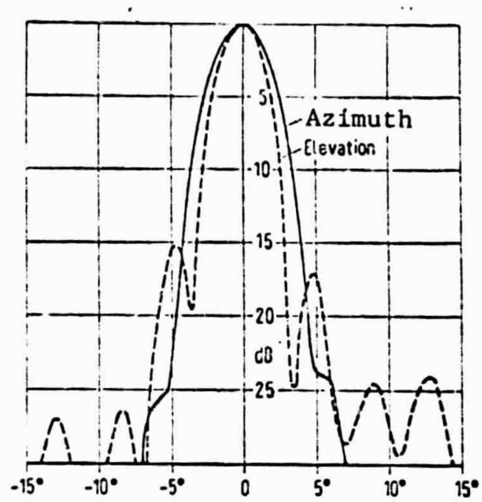

Figure 3.7. TE_{11} radiation characteristic of the parabolic horn antenna. Vertical polarization; f = 12.4 GHz.

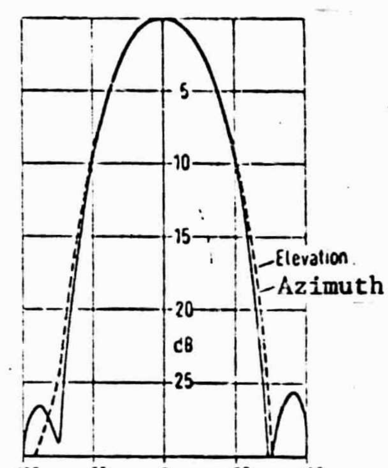

Figure 3.8. TE_{11}-TM_{11} radiation characteristic of the parabolic horn antenna b/a = 0.77; vertical polarization; f = 8.2 GHz, delay line length: l = 22 mm and l = 95 mm, respectively

The most important measurement results are summarized in Table 1. Table 2 contains measurement data for TE_{11} - TM_{11} radiation. Symmetrization of the radiation pattern was optimized for f = 8.2 GHz as shown in Figure 3.8. Additional emission of the TM_{11} wave and suitable choice of the amplitude ratio and phase of both wave modes results in a far-field characteristic in the antenna aperture with nearly complete rotational symmetry. The spread in the E-plane (elevation diagram) is adapted to the beam width in the H-plane. As expected, the radiation pattern in the H-plane (azimuthal diagram) remains almost unchanged by the TM_{11}-superposition. The sidelobe level in the elevation plane is simultaneously lowered from 17 dB to approximately 30 dB below the maximum of the main lobe. There is a gain

TABLE 1. Typical results of TE_{11}-far field measurements with parabolic horn antenna.

Measurement frequency	$f = 8{,}2$ GHz			$f = 12{,}4$ GHz		
Diagram width	3 dB	10 dB	20 dB	3 dB	10 dB	20 dB
Azimuth	6,0°	10,0°	13,3°	4,0°	7,0°	9,2°
Elevation	4,8°	7,8°	9,8°	3,4°	5,3°	9,2°

TABLE 2. Typical results of dual-mode far field measurements with a parabolic horn antenna.

Measurement frequency		$f = 8{,}2$ GHz			$f = 12{,}4$ GHz		
Diagram width		3 dB	10 dB	20 dB	3 dB	10 dB	20 dB
Phase delay section length 1 = 22 mm	Azimuth	6,0°	10,0°	13,3°	4,1°	7,0°	13,0°
	Elevation	6,0°	10,2°	14,1°	3,6°	5,9°	7,5°
Phase delay section length 1 = 22 mm	Azimuth	6,0°	10,0°	13,3°	4,8°	8,2°	11,0°
	Elevation	6,0°	10,2°	14,1°	3,2°	5,8°	11,5°

reduction due to the added TM_{11} radiation because of a beam broadening in the E-plane, but this drop is small due to strong sidelobe suppression. The measured gain reduction amounted to (0.25 ± 0.05) dB.

The bandwidth of this antenna system is also limited by the frequency dependence of the wave-mode converter and the phase of these modes at the antenna aperture. The beam widths in both orthogonal planes for constant phase delay section length (1 = 22 mm) and f = 8.6 GHz are almost identical down to approximately 15 dB below the maximum as shown in Figure 3.9. The pattern widens in the lower sections of the intensity diagram. A frequency increase to 9 GHz widens the pattern sufficiently to form a sidelobe with approximately 27 dB. The 10 dB pattern widths in the elevation and azimuth planes differ, however, by only 1.5°. A similar radiation characteristic is obtained for a frequency reduction to 7.9 GHz.

Similar results are obtained when the phase delay section length is altered instead of the frequency. The effect of the phase between

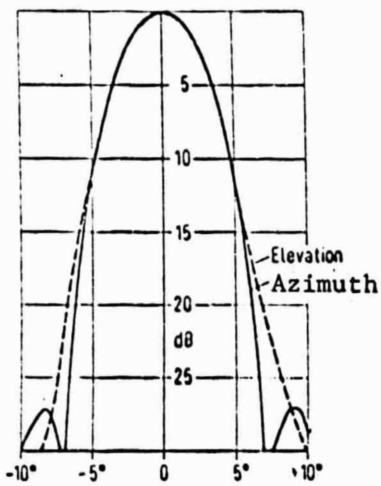

Figure 3.9. TE_{11}-TM_{11} radiation characteristic of the parabolic horn antenna b/a = 0.77; vertical polarization; f = 8.6 GHz, delay section: l = 22 mm.

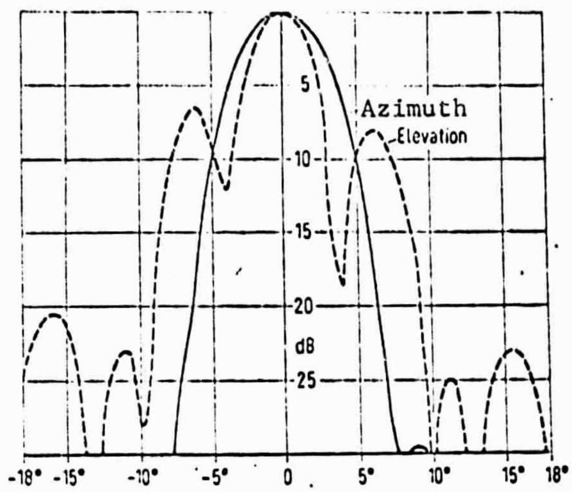

Figure 3.10. TE_{11}-TM_{11} radiation characteristic of the parabolic horn antenna. b/a = 0.77; vertical polarization; f = 8.2 GHz; delay system: l = 60 mm.

the two wave modes on the radiation pattern is shown in Figure 3.10 for the case of opposite phase (l = 60 mm) between the TE_{11} and TM_{11} waves in a parabolic horn aperture. The sidelobe level in the elevation plane has increased to approximately 6 dB. Similar characteristics are obtained for f = 10 GHz. A change in the phase delay section length (l = 22 mm) by full multiples of the interference wavelength for the TE_{11}-TM_{11}-wave mode combination at the optimum frequency (73 mm) to l = 95 mm results in a radiation field pattern with rotational symmetry.

When the delay section length is maintained at l = 22 mm and the frequency is increased further, then the conditions for TE_{11}-TM_{11} wave radiation again become more favorable. The effect of tube length change becomes smaller because of the larger interference wave length of the TE_{11}-TM_{11}-wave type combination. Figures 3.11 and 3.12 show distribution patterns for f = 12.4 GHz which were measured at delay section positions that produced a radiation pattern with rotational symmetry at f = 8.2 GHz. There is no significant difference compared to the TE_{11} patterns shown in Figure 3.7. With suitable frequency ranges and over a limited interval of phase delay section lengths it is therefore possible to control the radiation characteristics of the dual-mode antenna within certain limits over a signif-

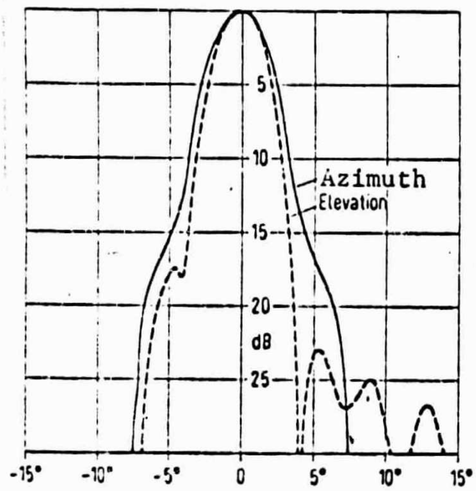

Figure 3.11. TE_{11}-TM_{11} radiation characteristic of the parabolic horn antenna. b/a = 0.77; vertical polarization; f = 12.4 GHz, delay system: l = 22 mm.

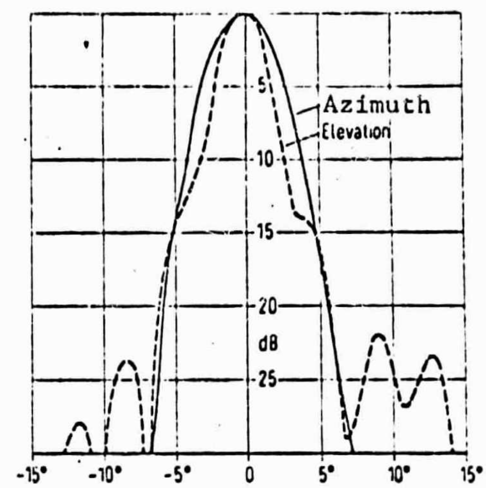

Figure 3.12. TE_{11}-TM_{11} radiation characteristic of the parabolic horn antenna. b/a = 0.77; vertical polarization; f = 12.4 GHz, delay system: l = 95 mm.

icantly larger frequency range. Certain restrictions must, however, be accepted. For example, a gain reduction of (0.6 ± 0.05) dB was measured against the parabolic horn antenna with TE_{11}-mode emission. In the evaluation of these restrictions one must, however, consider that the radiation characteristic of the parabolic horn antenna has been significantly improved in the frequency range near f = 8.2 GHz.

3.6 THE PARABOLIC HORN ANTENNA AS NEAR-FIELD FEED OF A CASSEGRAIN ANTENNA

Sidelobe suppression in the E-plane is of greater importance for the use of parabolic horn antennae as a directional antenna than for the rotational symmetry of the radiation distribution. A significant improvement may, however, be expected when the dual-mode principle is used in a parabolic horn exciter as the near-field feed of a Cassegrain antenna. The rotational symmetry of the energy distribution causes the receiver reflector in the near field to be illuminated with rotational symmetry. The near-field region is limited roughly by the Rayleigh distance $R = D^2/2\lambda$. An estimate of the attainable gain increase of the full system results in a value of approximately 0.5 dB for a 25 m antenna.

In order to determine the optimum receiver size and shape, one must measure the amplitude and phase distribution of the parabolic horn antenna at the receiver position in planes perpendicular to the emitter aperture. According to measurements on a parabolic horn antenna with conventional TE_{11} emission [5] we have placed the receiver reflector at a distance L = 0.27 R in front of the parabolic horn aperture for an optimum frequency of f = 8.2 GHz.

Figure 3.13 shows the amplitude distribution for TE_{11} emission. The aperture diameter is shown in Figure 13 and subsequent graphs in order to indicate the size of the receiver reflector. The different degrees of edge illumination of the receiver reflector in two orthogonal planes are clearly visible. The H-plane is focussed more strongly than the E-plane. A superposition of the TE_{11}-wave with the TM_{11}-wave approximates the E-plane focussing to that of the H-plane; nearly complete agreement is obtained as shown in Figure 3.14. A similar result is obtained for the phase distribution (Figure 3.15). Simultaneous emission of the TM_{11}-wave causes the phase fronts in the E and H planes to approach each other. The phase front is nearly flat near the center of the antenna aperture and diverges towards the edge. These measurements of the spatial phase front pattern show that the receiver reflector contour is parabolic only in the center and must be corrected in the outer region.

Figure 3.16 shows the amplitude and phase pattern of the TE_{11}-TM_{11} wave mode combination at f = 12.4 GHz, i.e. higher by a factor of 1.5. The distance between the plane of measurement and the aperture was maintained so that the frequency variation became L/R = 0.18. The resulting graphs are almost identical to the amplitude and phase characteristics of the TE_{11} wave. The phase pattern within the H-plane has, however, become less favorable. Measurements were made for delay section positions which produced optimum radiation patterns at f = 8.2 GHz. It is therefore possible to exert some control over the strong phase change between the two wave modes upon a frequency increase. As in the case of far-field measurements, it is again

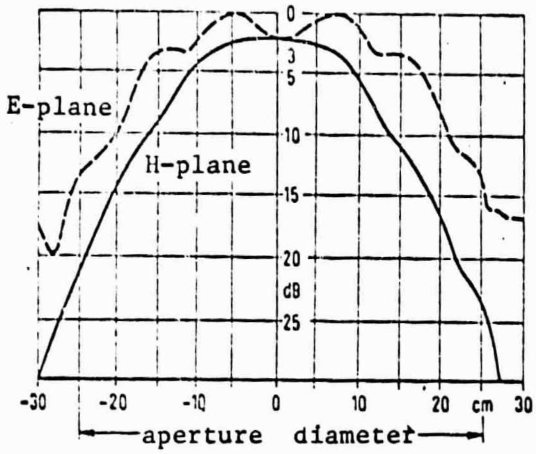

Figure 3.13. TE_{11}-near field characteristic for the parabolic horn antenna. L/R = 0.27; f = 8.2 GHz.

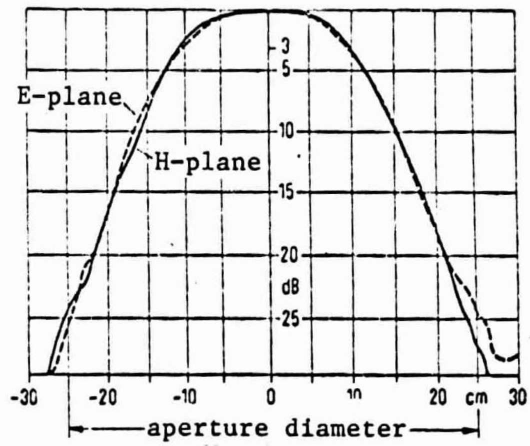

Figure 3.14. TE_{11}-TM_{11} near field characteristic of the parabolic horn antenna. L/R = 0.27; f = 8.2 GHz; l = 22 mm and l = 95 mm, respectively.

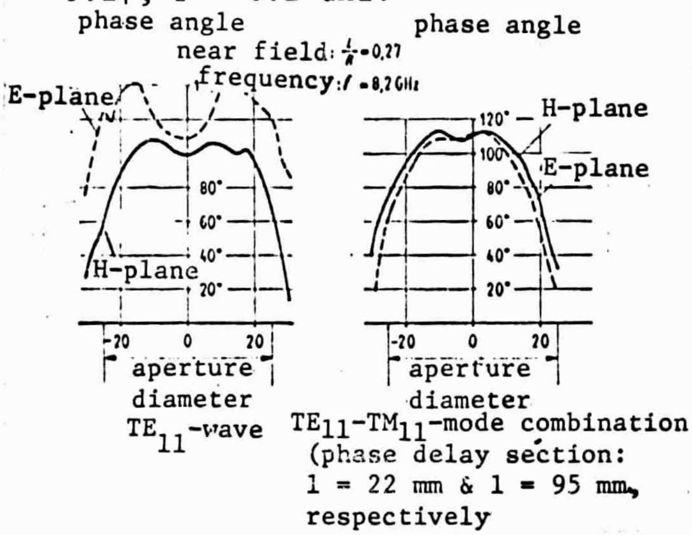

Figure 3.15. Phase distribution in front of the parabolic horn antenna aperture. L/R = 0.27; f = 8.2 GHz

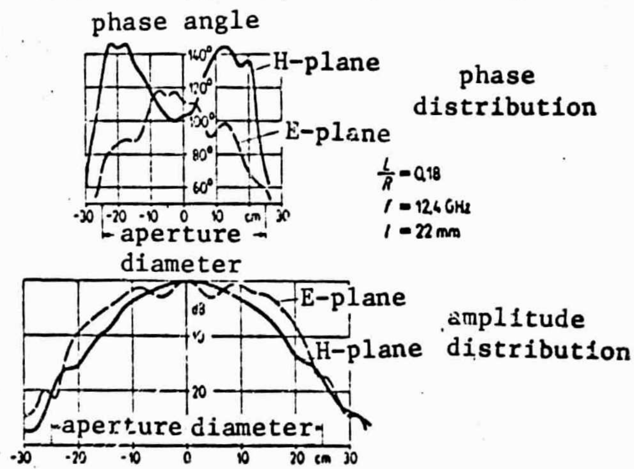

Figure 3.16. TE_{11}-TM_{11} radiation characteristic in front of the parabolic horn antenna aperture. L/R = 0.18; f = 12.4 GHz; l = 22 mm.

necessary to accept certain restrictions. The TE_{12}-wave is also excited by the cross-section discontinuity and may propagate at higher frequency ranges. This wave exerts a significant influence on the resulting amplitude and phase characteristics.

3.7 RADIATION CHARACTERISTIC OF TE_{01} AND TM_{01} DIRECTIONAL WAVES IN THE DUAL-MODE PARABOLIC HORN ANTENNA

The TM_{01} and TE_{01} directional characteristics were measured with suitable wave-mode selective coupling arrangements. Their function and mechanical construction have been described in [3]. The TM_{01} coupler is located behind the cross-section discontinuity in the narrow section of the waveguide, since the limiting frequency of the TM_{01} wave is smaller than that of the TM_{11} wave. An axial shift of the cross-section discontinuity did therefore not result in any change of the TM_{01} directional characteristic. The resulting radiation pattern is identical with the TM_{01} directional diagram of a parabolic horn antenna with conventional excitation.

The TE_{01}-wave has the same limiting frequency as the TM_{11} wave. It is therefore completely reflected at the cross-section discontinuity. Hence the de-coupling slits of the TE_{01} adapter are located where the wall currents of the resulting standing wave are largest. A detailed investigation of TE_{01}-de-coupling in a dual-mode system is described in [4]. An axial shift of the point of discontinuity by multiples of one-half of the wave-guide wave length for the TM_{01} wave results in a cyclic variation of the degree of TE_{01} de-coupling.

The directional diagram of a TE_{01} wave in Figure 17 is a typical example for the radiation characteristic of directional wave modes in a dual-mode parabolic horn antenna. The shoulders are steep and are located symmetrically with respect to the beam axis. The amount of damping at the minimum was out of range for the 35 dB meter which was used here. The most important part of the directional diagram is independent of the antenna position. A further important result is that the directions of minima in the TE_{01} and TM_{01} direc-

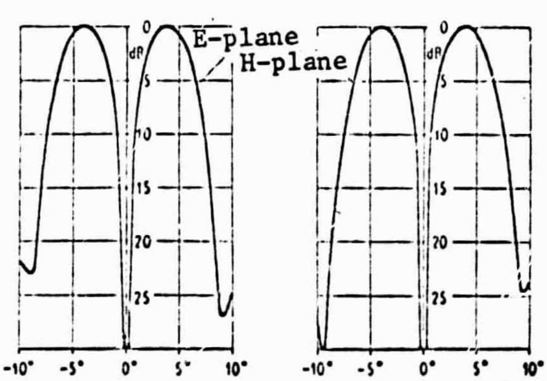

Figure 3.17. TE_{01}-far field characteristic of the TE_{11}-TM_{11} parabolic horn antenna. f = 8.2 GHz; l = 22 mm.

tional diagrams showed excellent agreement.

3.8 CONCLUSION

The present basic investigations showed that TE_{11} - TM_{11} mode emission allows us to build a Cassegrain antenna with very low noise at the receiver frequency and simultaneously good radiation properties at the transmission frequency, provided the cone aperture angle of the parabolic horn antenna can be made sufficiently large. The bandwidth for large cone aperture angles is essentially determined by the dispersion of TE_{11}- and TM_{11} waves in the common cylindrical phase delay section behind the cross-section discontinuity. It is thus possible to obtain values which are sufficient for practical applications. This approximation does not apply for small aperture angles. The slowly decreasing dispersion of phase velocity of wave modes in the cone section, together with the usual large length of the parabolic horn antenna, allow us to fulfill the required phase condition for rotationally symmetric radiation in the transmitter aperture only within a very narrow range of frequencies.

REFERENCES

1. Trentini, G. v. Feed systems for Cassegrain antennae. Frequenz 17, 1963, p. 491-499.

2. Potter, P. D. A new horn antenna with suppressed sidelobes and equal beamwidths. The microwave Journal, June 1963, p. 71-78.

3. Reitzig, R. Automatic tracking of antennas. Nachrichtentechnische Fachberichte 32, 1967, p. 45-51.

4. Reitzig, R. Application of the variational principle to the determination of the effect of small irregularities within a circular waveguide. Frequenz 22, 1968, p. 45-52.

5. Trentini, G. v., K. P. Romeiser and W. Jatsch: Design and electrical properties of the 25 m antenna of the ground station Raisting for communication links via satellite. Frequenz 19, 1965, p. 402-421.

The superposition of the TE11- and TM11-circular waveguide modes with the appropriate relative amplitude and phase in the aperture of a horn-reflector antenna causes beamwidth equalization and sidelobe suppression of from 17 dB to more than 30 dB in the electric plane. The TM11-mode is set up at the junction of two circular wave-guides of different cross-section. A theoretical analysis of the mode-conversion and the dimension of the cross-sectional discontinuity for the condition of a rotational-symmetric distribution of the radiation field are presented. In addition, measurements of the far-field radiation pattern and the near-field are presented. In addition, measurements of the far-field radiation pattern and the near-field distribution of the amplitude and the phase are given. The radiation characteristics of the TM01- and TE01- circular waveguide modes required for antennae tracking purposes are also investigated. Author